

Swelling–shrinkage measurements of bentonite using coupled environmental scanning electron microscopy and digital image analysis

G. Montes-H*

UMR 7517 ULP—CNRS, CGS, 1 rue Blessig, F-67084 Strasbourg, France

Received 12 August 2004; accepted 15 September 2004

Available online 11 November 2004

Abstract

The swelling clays have been proposed as engineered barriers in geological disposal systems for waste because these materials are assumed to build a better impermeable zone around wastes by swelling. However, the swelling potential of soils is also considered a prevalent cause of damage to buildings and constructions. For these reasons, it is fundamental to investigate the physicochemical and mechanical behavior of swelling clays. In the current study, the swelling–shrinkage potential (aggregates scale) was estimated using an environmental scanning electron microscope (ESEM) coupled with a digital image analysis (DIA) program (Visilog). In fact, the isolated aggregates of raw and cation-exchanged bentonite were directly observed at different relative humidities in an ESEM chamber. Then the “Visilog” software was used to estimate the percent augmentation of the aggregate surface as a function of time and as a function of relative humidity. This estimation allows for the calculation of the swelling–shrinkage potential (%) of bentonite. Finally, a kinetic model of first order was tested to fit the kinetic experimental data of swelling–shrinkage potential. The results show that ESEM–DIA coupling can be a powerful method of estimating the swelling–shrinkage potential of expansive clays. In addition, the exponential models fit well with the kinetic experimental data.

© 2004 Elsevier Inc. All rights reserved.

Keywords: Swelling–shrinkage; Kinetic; Bentonite; ESEM; Interlayer cations; Digital image analysis (DIA)

1. Introduction

The industrial and environmental uses of clays are expanding every year. For example, it is estimated that about 8 million tons of the bentonites were used in 1992 throughout the world [1]. One of the principal applications for bentonite is in drilling muds. However, it is widely used as a suspending and stabilizing agent and as an adsorbent or clarifying agent in many industries. Recently the swelling clays have been proposed as engineered barriers in geological disposal systems for waste because these materials are assumed to build up a better impermeable zone around wastes by swelling [2,3]. Unfortunately, the swelling soils are one of the most prevalent causes of damage to buildings and construction. The losses include severe structural

damage, cracked driveways, sidewalks and basement floors, heaving of roads and highway structures, condemnation of buildings, and disruption of pipelines and sewer lines [4,5]. This makes the estimation of the swelling–shrinkage potential of expansive clays in the laboratory very important. The methods available for the estimation of the swelling–shrinkage potential are grouped into two categories: physicochemical and mechanical methods. The common analytical techniques used in physicochemical methods are X-ray diffusion at small angles, X-ray diffraction, scanning transmission electron microscopy (STEM), and imbibition. On the other hand, the classic experimental techniques used in the mechanical methods are the consolidometer test and the soil suction test [6–8].

In the current study, the swelling–shrinkage potential (aggregates scale) was estimated using an environmental scanning electron microscope (ESEM) coupled with a digital image analysis (DIA) program (Visilog). In fact, the isolated aggregates of raw and cation-exchanged bentonite were di-

* Fax: +33-39024-0402.

E-mail address: montes@illite.u-strasbg.fr.

rectly observed at different relative humidities in an ESEM chamber. Then the Visilog software was used to estimate the percent augmentation of the aggregate surface as a function of time and as a function of relative humidity. This estimation allows the calculation of the swelling–shrinkage potential (%) of bentonite. Finally, a kinetic model of first order was tested to fit the kinetic experimental data on swelling–shrinkage potential [9–11].

2. Material and methods

2.1. MX80 bentonite

MX80 bentonite contains Na/Ca-montmorillonite (80%), quartz (6%), K-feldspars (2%), plagioclases (4%), carbonates (4%), mica (3%), and other minerals (1%) [12]. The bulk sample is composed of 86.1% of particles in a size range less than 2 μm , 8.8% in the range 2–50 μm , and 5.1% for sizes larger than 50 μm [13]. The specific surface area of the bulk sample was estimated at 33 m^2/g ($\pm 1 \text{ m}^2/\text{g}$) by applying the Brunauer–Emmet–Teller (BET) equation and by using 16.3 \AA^2 for the cross-sectional area of molecular nitrogen. For this estimation, a Sorptmatic 1990 instrument was used.

2.2. Samples preparation

The bulk samples of MX80 bentonite were treated separately with two concentrated solutions (1 N) of sodium and calcium chlorides, both with the same ionic force ($I = 2$). Twenty grams of MX80 bentonite were dispersed into 1 L of salt solution (1 N) at 60 °C. This suspension was vigorously stirred with magnetic agitation for 1 h at 60 °C. Then the cation-saturated clay was separated by centrifugation (15 min at 13,000 rpm) and decanting the supernatant solutions. This process was repeated three times. The cation-saturated bentonite was then washed three to four times with distilled water until the AgNO_3 test for chloride was negative. This method was used by Seung Yeop Lee and Soo Jin Kim [14] and Giora Rytwo [15].

The cation-saturated bentonite was subsequently dried for 48 h at 60 °C and finally ground for 2 min.

Finally, the raw and cation-saturated bentonite were dried for 24 h at 110 °C and placed in plastic desiccators (2 L) in order to keep the hydration state of samples constant using silica gel.

2.3. ESEM methodology

For all environmental scanning electron microscope investigations, an XL30 ESEM LaB6 (FEI and Philips) was used with a gaseous secondary electron detector (GSED) to produce a surface image. This microscope is also equipped with a cooling stage to control the sample temperature.

2.3.1. Kinetic procedure

Drying. The chamber pressure and sample temperature are respectively fixed at 2.3 Torr and 50 °C. In this case, the relative humidity of the surrounding sample is 2.5% according to the water phase diagram. The sample is maintained at these “reference conditions” for about 15 min, and an image of an aggregate of interest is chosen and stored in the hard disk of the control PC.

Swelling. The chamber pressure and the sample temperature are simultaneously set at 8.2 Torr and 9 °C, respectively, and images were immediately taken approximately every 30 s for 10 min.

Shrinkage. Here the chamber pressure and sample temperature are again brought back under reference conditions ($P = 2.3 \text{ Torr}$ and $T = 50 \text{ °C}$). The image acquisition is also done as a function of time for 10 min.

This kinetic procedure of swelling–shrinkage was carried out only on the raw-bentonite aggregates at nine relative humidities (95, 90, 85, 80, 75, 70, 65, 60, and 55%).

2.3.2. Equilibrium-state procedure


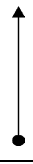
Each sample was submitted to hydration and then a dehydration cycle, with progressively increasing and decreasing relative humidity.

Drying. This stage is identical to the kinetic procedure described above.

Swelling. This manipulation was achieved at a constant sample temperature of 9 °C. Then the progressive sample hydration was performed by increasing the chamber pressure until water oversaturation of the sample was achieved. The water oversaturation of aggregates was observed between 80 and 95% relative humidity.

The pressures shown in the Table 1 were used to keep a constant relative humidity of surrounding sample in the ESEM chamber. In each step of chamber pressure an image of interest was taken after 5 min. This time was considered as equilibrium time and was previously estimated by kinetic manipulations.

Table 1
Pressures used to control the constant relative humidity of the surrounding sample in the ESEM chamber at a constant temperature of 9 °C

	Chamber pressure (Torr)	Relative humidity (%)	
Swelling 	2.6	30	Shrinkage 
	3.4	40	
	4.3	50	
	5.2	60	
	6.0	70	
	6.4	75	
	6.9	80	

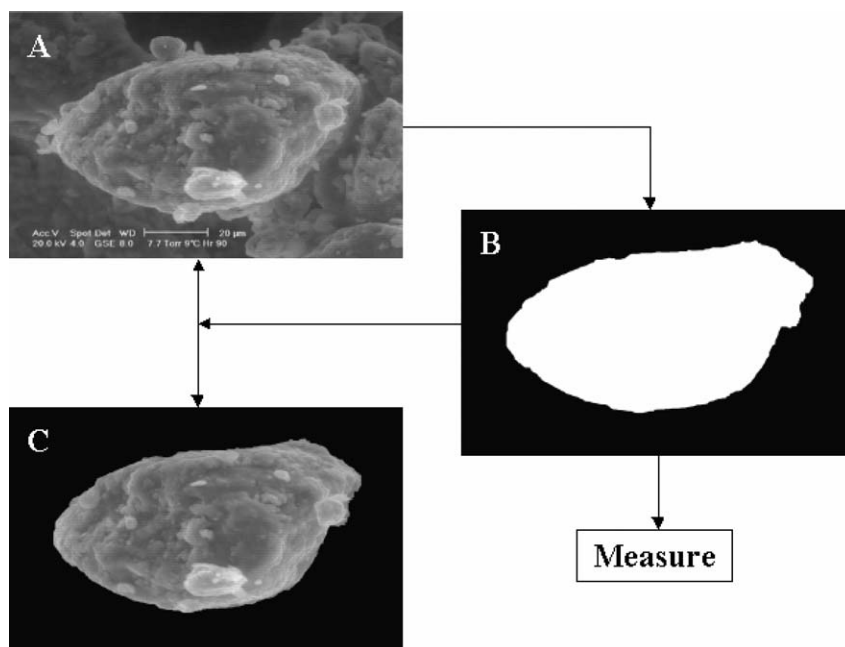


Fig. 1. Digital image analysis methodology: (A) ESEM image; (B) image binarization and isolation of the surface “aggregate” of interest; (C) image reconstitution and control verification (after [10]).

Shrinkage. This stage was done inversely from that of swelling. Here the chamber pressure was progressively decreased until the reference conditions were reached (see Table 1). The sample temperature was always kept at 9 °C.

2.4. DIA methodology

Digital image analysis consists of isolating an area of interest with Visilog 5.3 software. In this study the area of interest was always an aggregate.

Generally the ESEM images have a sufficient density contrast to isolate the area of interest by applying a simple gray level threshold. To minimize the experimental error of the surface measure, the same procedure, i.e., digital image analysis, was applied manually five times. In addition each analysis was visually controlled by the reconstitution of a binary image (Fig. 1).

The ESEM images of the test section occupied about 1424×968 pixels, and in all measurements the same gray-level range, 0–256, was considered.

3. Results and discussion

3.1. Experimental data

The experimental swelling–shrinkage data are derived from digital image analysis, bidimensional analysis. The results are shown as surface augmentation and/or diminution as functions of time (kinetic curves) or as functions of relative humidity (isotherms). The swelling–shrinkage percent-

age is then estimated by

$$S = \frac{S_{t-RH} - S_i}{S_i} 100, \quad (1)$$

where S_{t-RH} represents the surface area at an instant time t or in a RH equilibrium state (μm^2) and S_i represents the initial surface area of the dry sample (μm^2).

The experimental kinetic curves and experimental isotherms of swelling–shrinkage potential of bentonite (aggregate scale) are shown in Figs. 2 and 3.

3.2. Measurements precision

The average standard deviation obtained after five repeated surface area measurements was considered as an estimate of the absolute error on swelling–shrinkage,

$$E = \frac{s(\bar{q})}{S_i} (200 + S), \quad (2)$$

where $s(\bar{q})$ is the average standard deviation, S_i is the initial surface, and S is the swelling–shrinkage percentage.

The absolute error remains relatively low. However, the error is always more significant at low relative humidity (Fig. 4).

3.3. Fitting of kinetic curves

3.3.1. Swelling

The experimental data were fitted using a kinetic model of first order,

$$\frac{dw}{dt} = k(w_M - w). \quad (3)$$

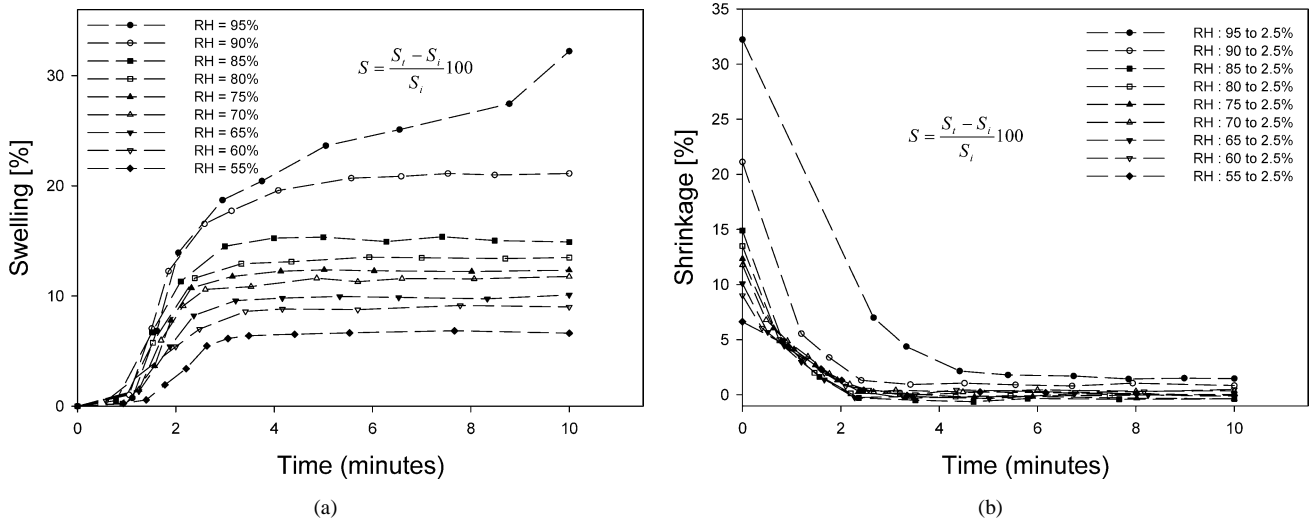


Fig. 2. Kinetic experimental data of the swelling (a) and shrinkage (b) of raw-bentonite aggregates at nine different relative humidities

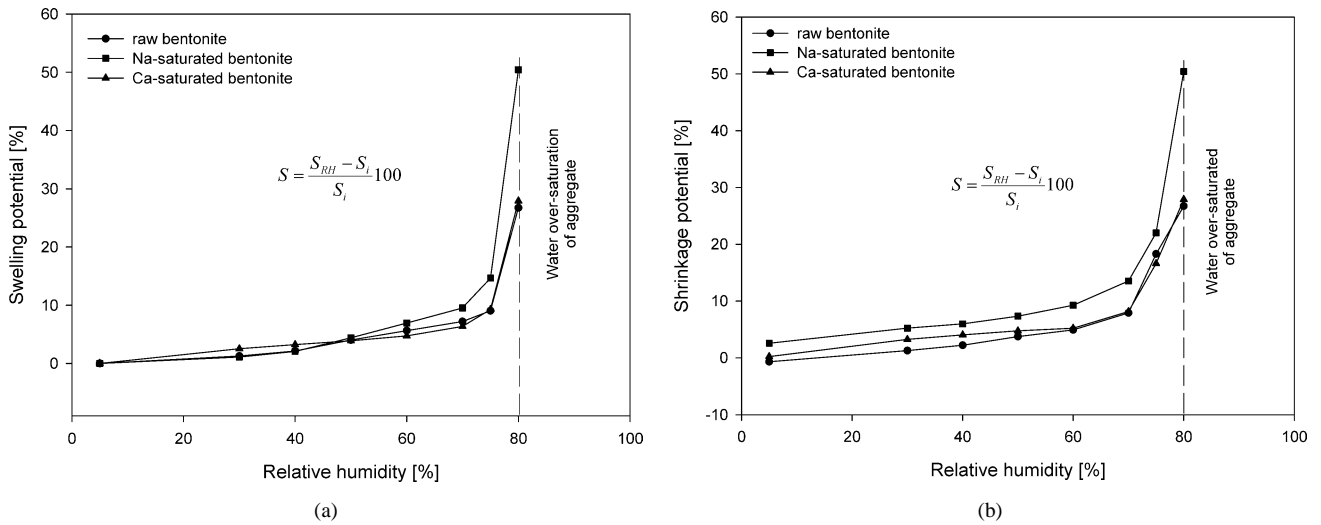


Fig. 3. Swelling (a) and shrinkage (b) potential isotherms of raw and cation-saturated bentonite by ESEM-DIA.

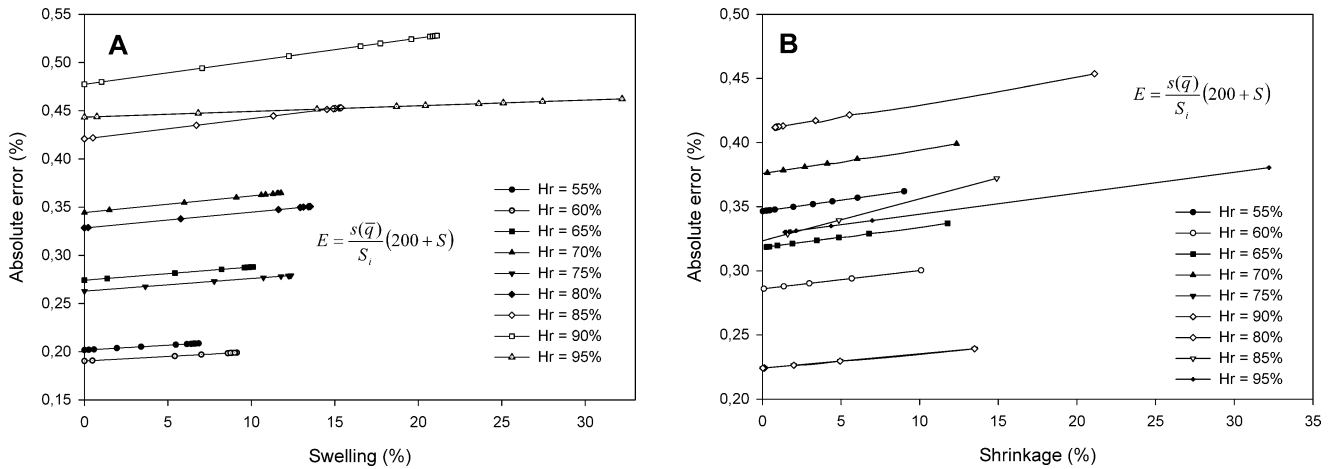


Fig. 4. Absolute error behavior: (A) swelling; (B) shrinkage.

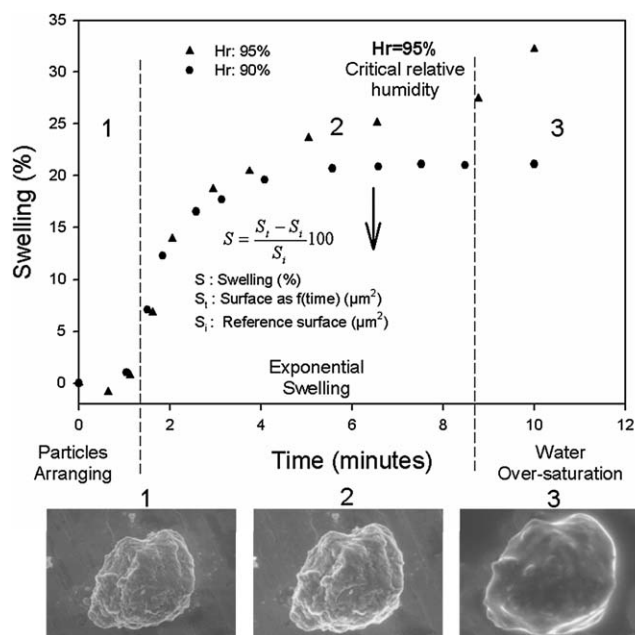


Fig. 5. Swelling kinetics of raw bentonite aggregate scale using ESEM-DIA coupling.

This kinetic model represents the volume augmentation as a function of time up to an asymptotic maximum of time. The integral form is represented by an exponential equation:

$$w = w_M(1 - \exp(-kt)). \quad (4)$$

This equation can only be applied when the volume varies. Unfortunately, the measurement estimated in this study corresponds to surface area variations and not to volume variations. If we consider that the swelling–shrinkage of the bentonite is equidimensional on an aggregate scale, Eq. (4) can be written in terms of surface:

$$S = S_M(1 - \exp(-kt))^{2/3}. \quad (5)$$

On the other hand, the experimental data show that the swelling kinetics of raw bentonite aggregates can be defined by three stages (Fig. 5). The first stage is very difficult to model, because of the random arrangement of the particles in the initial water adsorption. In general this stage is characterized by a nonswelling feature and sometimes by an aggregate contraction. The second stage presents a high swelling during the first minute, after which the swelling decreased gradually up to an asymptotic maximum of time. This stage may be modeled by an exponential equation (5). The third stage, called “aggregate water oversaturation,” is only presented at a critical relative humidity between 80 and 95%. The first and second stages were also identified by the mechanical methods for other expansive clays [4,16].

The final equation, to fit only the second stage of bentonite swelling, is then

$$S = S_M(1 - \exp(-k(t - t_0)))^{2/3}, \quad (6)$$

with S_M the maximum swelling (%), k the coefficient of swelling (1/min), and t_0 the initial time of the exponential swelling.

3.3.2. Shrinkage

The shrinkage behavior makes up one stage, which may be modeled by an exponential decay model. The final equation in terms of surface is

$$D = S_M(\exp(-k_d t))^{2/3}, \quad (7)$$

with S_M the maximum swelling (%) and k_d the coefficient of shrinkage (1/min).

The fitting parameters for kinetic curves of swelling and shrinkage are summarized in Tables 2 and 3. These parameters were estimated by nonlinear regression using a least-squares method. In addition, Fig. 6 shows a example of experimental data fitting at 90% relative humidity.

The exponential models used to fit the swelling and shrinkage are very well correlated with the experimental data, since the estimated coefficients of nonlinear regression are close to 1 (Tables 2 and 3). This may be an indirect reason to confirm that the swelling–shrinkage is effectively equidimensional. The second reason to confirm the equidimensionality of the swelling–shrinkage “aggregate scale” is done by digital image analysis, which shows a linear correlation between the width and the length of the aggregate (Fig. 7).

Table 2

Fitting kinetic parameters for Bentonite swelling at eight relative humidities: nonlinear regression by least-squares method [9]

Humidity (%)	Fitting parameters			Regression coefficient
	S_M (%)	k (1/min)	t_0 (min)	R
90	20.99	0.88	1.24	0.9978
85	15.21	1.33	1.26	0.9955
80	13.43	1.50	1.31	0.9992
75	12.32	1.75	1.46	0.9983
70	11.51	1.66	1.41	0.9936
65	9.91	1.84	1.60	0.9980
60	9.01	1.23	1.50	0.9953
55	6.79	1.13	1.65	0.9841

Table 3

Fitting kinetic parameters for Bentonite shrinkage at eight relative humidities: nonlinear regression by least-squares method [9]

Humidity (%)	Fitting parameters		Regression coefficient
	S_M (%)	k (1/min)	R
90 → 2.5	21.04	1.61	0.9940
85 → 2.5	14.95	2.16	0.9954
80 → 2.5	13.53	2.05	0.9988
75 → 2.5	12.40	1.68	0.9959
70 → 2.5	11.71	1.53	0.9956
65 → 2.5	10.20	1.77	0.9932
60 → 2.5	9.05	1.40	0.9930
55 → 2.5	6.93	1.12	0.9784

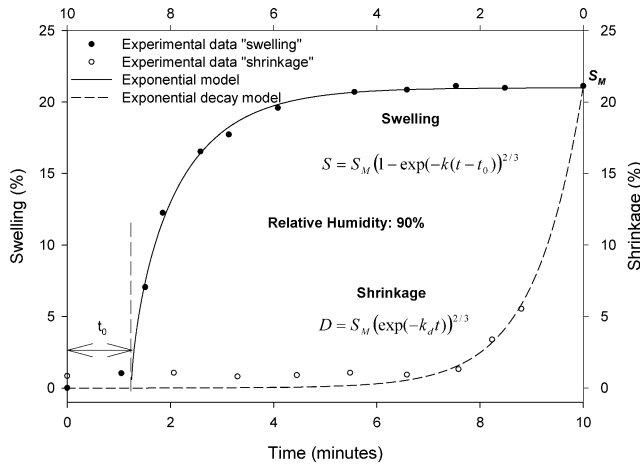


Fig. 6. Swelling–shrinkage cycle of raw bentonite at 90% relative humidity. Experimental data fitted by exponential models.

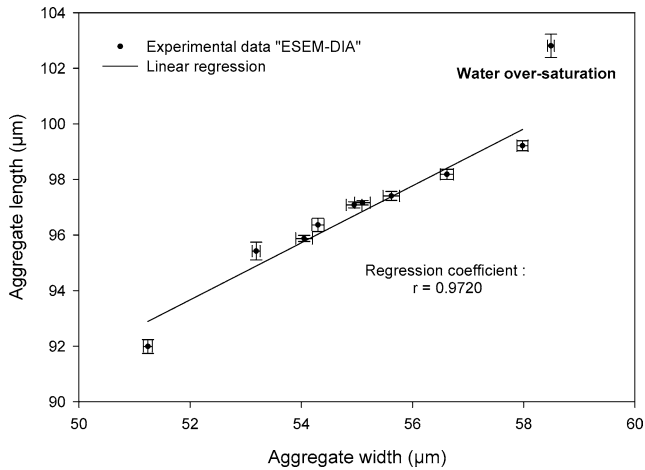


Fig. 7. Aggregate width and length correlation for swelling–shrinkage. Estimation by digital image analysis (DIA).

3.4. Comments on swelling–shrinkage isotherms

The swelling–shrinkage isotherms at 9 °C are shown in Fig. 3. It is clear that the swelling and shrinkage potential is governed by the relative humidity and by the nature of the interlayer cation. For example, globally Na-saturated bentonite presents an excellent capacity to swell while Ca-saturated bentonite swells less significantly at high relative humidities (>0.5). The raw bentonite presents an intermediate swelling–shrinkage potential because of the montmorillonite with mixed Na–Ca interlayer filling.

Finally, a Cartesian system was used to correlate the amount of adsorbed water and the swelling potential. This diagram shows a nonlinear correlation (Fig. 8). For this reason, a swelling-to-amount of adsorbed water ratio was calculated for low, medium, and high relative humidity (30, 50, and 75%, respectively) (Table 4). This basic approach must be considered with care because the amounts of adsorbed water and swelling potential were estimated separately by different analytical methods with different scales.

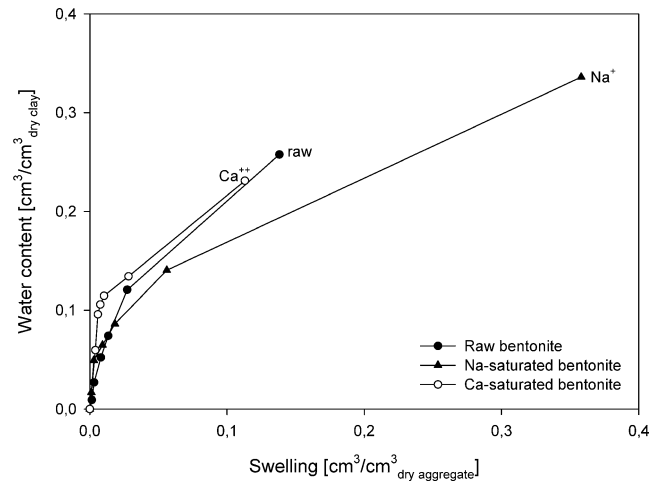


Fig. 8. Amount of adsorbed water and swelling potential correlation for raw and cation-saturated bentonite. The swelling potential was considered equidimensional to aggregate scale (corrected data from Fig. 7 [11]).

Table 4

The swelling-to-amount of adsorbed water ratio for low, medium, and high relative humidity: corrected data from Table 3 [11]

Sample	Swelling/amount of adsorbed water ratio		
	Low (RH 30%)	Medium (RH 50%)	High (RH 75%)
MX80 raw	0.1605	0.1558	0.2260
MX80-Na	0.0715	0.1442	0.3996
MX80-Ca	0.0681	0.0730	0.2106

4. Conclusions

Three main conclusions are given here.

First, the results show that coupling environmental scanning electron microscopy (ESEM) with digital image analysis (DIA) is a powerful method of estimating the swelling–shrinkage potential of expansive clays. The main advantage of this method is the rapidity with which one obtains qualitative and quantitative results. However, this method allows only estimation of the free swelling–shrinkage potential in the sample chamber.

Second, thanks to direct observations with ESEM, it was possible to identify three steps for swelling kinetics: (1) particle arrangement; (2) exponential swelling; (3) water over-saturation. In addition, the exponential models and the digital 2D image analysis confirm that the swelling–shrinkage potential of the MX80 bentonite is equidimensional aggregate scale.

Third, the swelling potential is governed by the relative humidity and by the nature of the interlayer cations. For example, globally the Na-saturated bentonite has an excellent capacity to swell, while the Ca-saturated bentonite swells less significantly at high relative humidities (>0.5). The raw bentonite presents an intermediate swelling–shrinkage potential because of the montmorillonite with mixed Na–Ca interlayer filling.

Acknowledgments

The authors are grateful to the National Council of Science and Technology, Mexico, and Louis Pasteur University, France, for providing a financial grant for this work.

References

- [1] H.H. Murray, *Appl. Clay Sci.* 17 (2000) 207.
- [2] R. Pusch, *Clay Miner.* 27 (1992) 353.
- [3] A. Al-Tabbaa, T. Aravinthan, *Waste Manage.* 18 (1998) 9.
- [4] A.A. Al-Rawas, *Eng. Geol.* 53 (1999) 327.
- [5] A.A. Al-Rawas, G. Ingeborg, A. McGown, *Eng. Geol.* 50 (1998) 267.
- [6] P. Parcevaux, Ph.D. thesis, Pierre et Marie Curie University, Paris, 1980.
- [7] S.A. Waddah, S.A. Waddah, A.A. Khalid, S.A. Mohammed, *Appl. Clay Sci.* 15 (1999) 447.
- [8] H. Komine, N. Ogata, *Can. Geotechnol. J.* 31 (1994) 478.
- [9] G. Montes-H, Ph.D. thesis, Louis Pasteur University, Strasbourg, 2002.
- [10] G. Montes-H, J. Duplay, L. Martinez, C. Mendoza, *Appl. Clay Sci.* 22 (2003) 279.
- [11] G. Montes-H, J. Duplay, L. Martinez, Y. Geraud, B. Rousset-Tournier, *Appl. Clay Sci.* 23 (2003) 309.
- [12] E. Sauzeat, D. Guillaume, A. Neaman, J. Dubessy, M. François, C. Pfeiffert, M. Pelletier, R. Ruch, O. Barres, J. Yvon, F. Villiéras, M. Cathelineau, Technical Report ANDRA CRP0ENG 01-001, 2001.
- [13] A. Neaman, M. Pelletier, F. Villiéras, *Appl. Clay Sci.* 22 (2003) 153.
- [14] Y.L. Seung, J.K. Soo, *J. Colloid Interface Sci.* 248 (2002) 231.
- [15] R. Giora, *Clays Clay Miner.* 44 (2) (1996) 276.
- [16] S. Wild, J.M. Kinuthia, G.I. Jones, D.D. Higgins, *Eng. Geol.* 51 (1999) 257.